Instrument for Airborne Remote Sensing of Transmission Pipeline Leaks

Final Report
August 2004

Submitted by

Thomas A. Reichardt, Sanjay Devdas, and Thomas J. Kulp
Diagnostics and Remote Sensing Department
Sandia National Laboratories
P.O. Box 969, MS 9056
Livermore, CA 94551

and

Wayne Einfeld
Environmental Monitoring and Characterization Department
Sandia National Laboratories
P.O. Box 5800, MS 0755
Albuquerque, NM 87185

This work was sponsored by

The Strategic Center for Natural Gas, Natural Gas Infrastructure Reliability Program, National Energy Technology Laboratory (NETL), DOE Office of Fossil Energy

Abstract

The pipeline industry would benefit considerably from the development of systems that could provide early warning capabilities for major pipeline integrity and safety issues indicated by leaks. In 2002 we assessed the requirements of optically based approaches for locating pipeline leaks remotely from airborne platforms. We chose the optimum configuration and selected the major system components for an instrument. In 2003 we took this effort to the next stage by designing and constructing a ground-based instrument with the necessary performance requirements for airborne remote sensing of pipeline leaks. With this prototype, we demonstrate methane plume detection at standoff distances of up to 100 m. Potential improvements are discussed which would improve the instrument performance – extending the detection range to 200 m, a standoff distance appropriate for a low-flying aircraft.

Table of Contents

List of Figures

1. Overview of Problem

The detection of gas leaks represents a critical operation performed regularly by the gas industry to maintain the integrity and safety of its vast network of piping, both above and below the ground. Below-ground piping includes approximately 400,000 miles of transmission pipelines and 1.4 million miles of distribution piping, while above-ground piping is located mainly at about 750 gas processing plants and some 3000 compressor stations. Whether addressing above or below ground gas sources, leak surveillance with state-of-the-art gas detectors can be a time-consuming operation of uncertain effectiveness.

For surveys of buried piping, state-of-the-art natural gas leak detectors employ a flame ionization detector (FID). A sampling pump in the unit continuously withdraws, or "sniffs," samples of the ambient air and delivers them through a sampling probe to the flame ionization sensor itself. The surveyor scans the ground, carrying the sampling probe barely above ground level. The probe must be brought fairly close to the leak vent to sample detectable quantities of gas. To find a leak quickly the surveyor must possess enough experience to know where to look. Complicating matters somewhat is the underground migration of leaking gas from buried pipes, causing the gas to reach the surface at some location often not apparent to the surveyor. Leak surveys with an FID can cover 8-10 miles per day in the man-portable mode, and slightly more in a vehicle-mounted mode. As an alternative to using an FID, low-flying aircraft are sometimes used to discern discolored vegetation caused by the gas leaks. This technique obviously cannot be used effectively in areas without sufficient vegetation, such as the desert and steppe areas or during the winter.

2. New Detection Technology

Based on these considerations, it would be desirable to develop a remote pipeline inspection instrument that could detect the leak remotely without physically sampling the air above the leak. Such a system might be implemented on a low-flying aircraft such as those used routinely for inspection of third-party infringement and discolored vegetation. In comparison to sampling probes, remote detection technologies possess several advantages:

- They provide the potential for faster monitoring, and more frequent inspection for leaks (as caused by external infringements, material fatigue, etc.).
- By visualizing the entire leak rather than sampling a particular volume of air, they allow for more accurate pinpointing of the leak location, decreasing pipe excavation costs once the leak is detected.
- They allow a more complete and effective coverage of pipeline right-of-ways where leaks might migrate.
- They depend less on operator experience and judgment for leak detection.
- They provide the ability to monitor inaccessible, or "over the fence," areas.

3. Review of Previous Work

There are two alternatives for remote infrared sensing techniques: (1) active detection, which requires illuminating the scene with a light source, usually a laser, that is absorbed by the target gas, and (2) passive detection, which relies on detecting radiative transfer due to a temperature and/or emissivity difference that usually exists between the background and the target cloud. While passive methods allow nearly unlimited range with a simple instrumental configuration, these methods rely upon a temperature difference between the plume and the ground surface

below it. Active detection removes the thermal constraint, but requires a laser and a relatively lower operational range. In 2002 we assessed the requirements of active and passive approaches to detect gas leaks remotely from airborne platforms. We predicted leak concentrations and geometries, calculated detection sensitivities for active and passive approaches, and experimentally confirmed performance predictions.[1] For passive detection, we examined the signal source term, measuring temperature differences between the ground and the air under different weather conditions. We were particularly interested in achieving the sensitivities required for detecting natural gas at a level desired by industry. Results showed that an active system would be optimum for deployment from a low-flying aircraft.

4. Active Detection

Methane plumes are detected by active methods when they absorb backscattered infrared (IR) radiation in a laser-illuminated scene (see Figure 1). The source term for active detection is a function of the concentration-length product of the target plume as well as the reflectivity of the background scattering surface. To maximize the laser attenuation by the target plume, the spectral profile of the laser must be narrower than the methane absorption linewidth and must be centered at the peak of the strongest absorption line that is not affected by interfering species. The strongest absorption band in the mid-IR is the υ_3 rovibronic band centered at ~3018 cm^{-1}. The optimal absorption feature in that band was found to be at 3057.7 cm^{-1}. Figure 2 contains a plot of a portion of the υ_3 band including this feature, calculated for a single pass through a methane plume density of 10 ppm-m. The calculation also assumed the presence of the only significant interferent (water vapor) present at a density of 0.038 atm-m. This concentration of methane will produce a roundtrip optical depth of 0.10 and will not overlap significantly with water vapor.

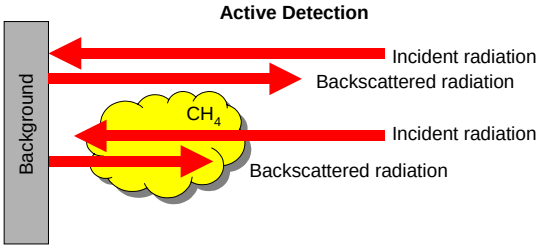

Figure 1. Active detection of gas plumes.

[1] T. A. Reichardt, S. Devdas, T. J. Kulp, and W. Einfeld, "Evaluation of active and passive gas imagers for transmission pipeline remote leak detection," Final report, SAND2003-8155W, available at http://www.netl.doe.gov/scng/projects/transmission/ngi/psr/pubs/psrFEW01-011123%202002%20Final%20Report.pdf.

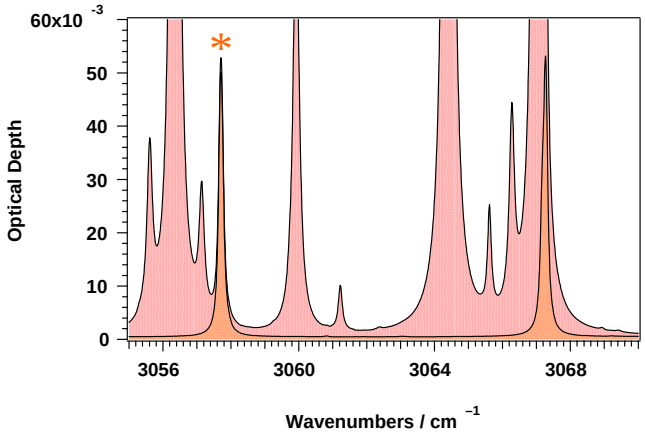

Figure 2. Spectrum of 10 ppm-m methane in 0.038 atm-m water vapor. The features in the forefront represent the absorption of methane while the features in the background represent the total absorption (methane plus water vapor).

Variation of the background surface reflectivity often limits the sensitivity of laser-backscatter measurements. The sensitivity of the instrument is limited by the minimum signal change that the detection algorithm can perceive. In a high-contrast scene the dynamic range must be scanned across a wide range of return signals to display the background scene image and the varying reflectivity of the background can mask the detection of a gas. This limitation can be overcome by using differential detection.[2] For differential detection, the scene is illuminated at two wavelengths: one corresponding to the peak of the methane absorption feature (termed the "on-wavelength") and one tuned away from the absorption feature (termed the "off-wavelength"). The column integrated methane concentration is calculated by taking the natural logarithm of the ratio of the on-wavelength signal to the off-wavelength signal. This effectively eliminates image features in the background, increasing the visibility of the methane column density. In practice, the wavelength of a pulsed laser source is dithered on and off the methane absorption feature for every other laser firing. The ln-ratio of the two successive laser pulses on and off the absorption feature is then calculated to determine the path-averaged methane concentration. From Figure 2, we expect that a laser spectrally narrower than the absorption feature will experience a round trip two-pass absorption of 1% per 1 ppm-m in the weak-absorption limit.

5. Design Parameters for Airborne Platform

For analysis of airborne remote leak detection, we will begin with the operational parameters of the low-flying aircraft used to discern discolored vegetation. This is illustrated in Figure 3. It was reported by industrial representatives that aircraft fly at an altitude of ~200 m at a speed of ~120 mph for detection of discolored vegetation. For remote optical detection of methane, we assume that we will probe a 10-m side-to-side area at a resolution of 0.5-m (Figure 4).

Remote detection of transmission pipeline leaks will likely require sweeping the detector field-of-view (FOV) over the area of interest to acquire an image of the integrated methane concentration between the aircraft and the ground surface. For active detection, this can be accomplished by either dithering a laser beam back and forth across the field of view (often

[2] P. E. Powers, T. J. Kulp, and R. Kennedy, "Demonstration of differential backscatter absorption gas imaging," Appl. Opt. 39, 1440-1448 (2000).

referred to as line scanning, see Figure 5a) or by spreading the laser beam so that it encompasses the necessary field of view (referred to as pushbroom acquisition, see Figure 5b). Because of the speed of airborne travel, the acquisition must be performed at a rapid rate to cover the required ground space within the area of interest. For a raster-scanning measurement at 120 mph, the FOV must be swept between measurement pixels at a rate of 2140 Hz. It is likely that an initial prototype instrument would be deployed without scanning, and instead acquire a single line-of-sight; this would lower the data rate by a factor of 20 to 107 Hz.

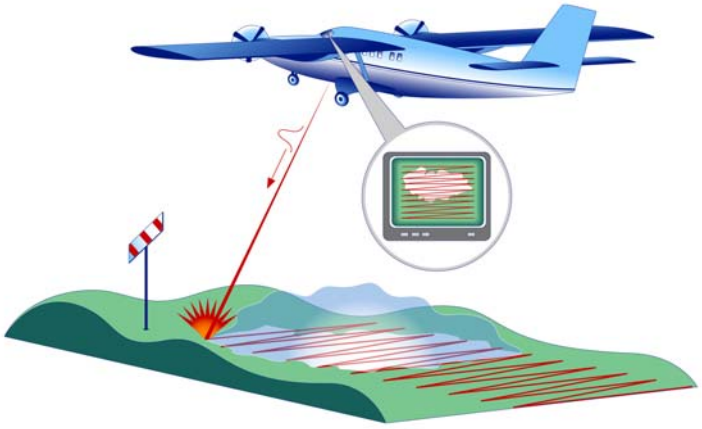

Figure 3. Airborne platform for detection of gas leaks

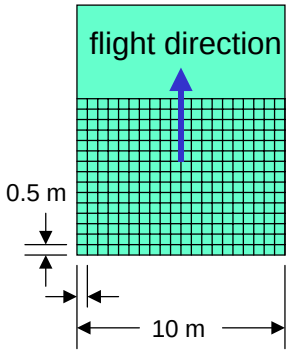

Figure 4. Detection field-of-view and resolution required for airborne detection.

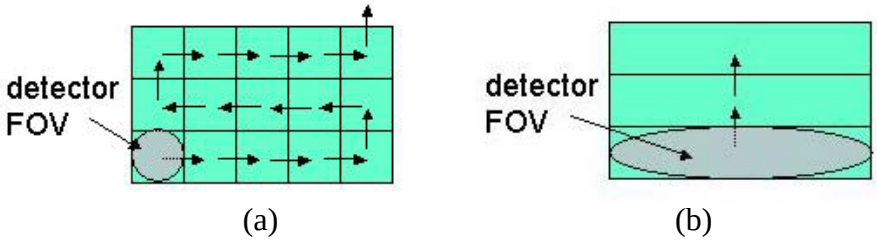

Figure 5. Detection scenarios: (a) raster scanning of FOV, (b) pushbroom acquisition.

6. Instrument Description

The instrument is comprised of two tiers: the top tier houses the light source while the bottom tier houses the receiver. The instrument is deployed on a mobile lever arm and be directed through either the side-viewing port or rear-viewing port in our mobile optical laboratory pictured in Figure 6. We can divide the discussion of the instrument into its three basic physical components: (1) the pump laser source, (2) the wavelength conversion device, and (3) the detector and amplifier used to sense the backscattered signal. Below we describe each of these components more fully. Some of the details of the components, however, are proprietary. Therefore abbreviated descriptions will be given.

Figure 6. Photographs of mobile optical laboratory. The photograph at the left displays the entire truck, while to the right the instrument is shown looking out of the side viewing port.

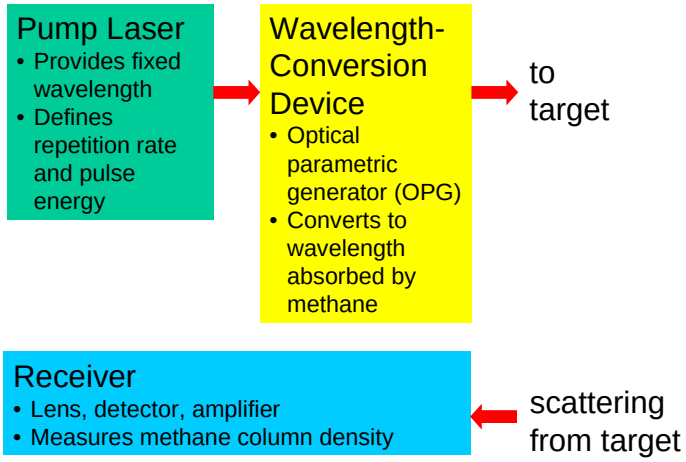

Figure 7. Instrument components.

Pump Laser

An appropriate pump laser is not available commercially, necessitating that we build our own laser source. We have decided to divide the pump laser into two components, a (1) master oscillator and a (2) power amplifier. The master oscillator defines the temporal stability, spectral

quality, and spatial quality of the pump laser. The power amplifier increases the pulse energy to the required magnitude while preserving the laser beam qualities of the master oscillator. A detailed description of the pump laser is planned for a future publication.

Wavelength-Conversion Device

The wavelength conversion device is a diode-seeded optical parametric generator (OPG).[3,4] This device is a PPLN (periodically poled lithium niobate) crystal that splits the laser light from the 1064-nm pump beam into two other beams, one at 1.58 μm (termed the signal beam) and one at 3.3 μm (termed the idler beam). The device is seeded with a distributed feedback diode (DFB) laser at 1.58 μm. The seeding is used to spectrally narrow the light emitted by the OPG as well as to control the exact wavelength of emitted light. The exact wavelength of the output photons is determined by setting the wavelength of the DFB laser via an adjustment of its drive current or its temperature. The tuning of the 3270.4 nm output relative to the peak absorption of methane is determined by the intensity of the beam transmittance through the miniature methane cell as measured by an InAs detector. Included with the InAs photodiode is signal amplification and sampling electronics.

Receiver

The receiver is composed of an f#/1 lens and an InAs detector to measure the 3.3-micron backscatter. Included with the InAs photodiode are signal amplification and sampling electronics.

7. Long-Distance Testing

We developed a portable leak generator (Figure 8) that was deployed at a distance remote from the mobile optical laboratory. Controlled plumes were released in a field for demonstration of detection limits. The plume generator is composed of a Sandia-built blower, a methane bottle, and an Environics flow controller, and it is powered by a portable Honda generator. An independent measurement of the flow rate (with a Gilibrator volumetric flow meter) confirms accuracy in the flow rates reported.

[3] T. A. Reichardt, R. P. Bambha, T. J. Kulp, and R. L. Schmitt, "A frequency-locked, injection-seeded, pulsed narrowband optical parametric generator," Appl. Opt. **42**, 2564-3569 (2003).

[4] M. Rahm, U. Bäder, G. Anstett, J. –P. Meyn, R. Wallenstein, and A. Borsutzky, "Pulse-to-pulse wavelength tuning of an injection seeded nanosecond optical parametric generator with 10 kHz repetition rate," Appl. Phys. B **75**, 47-51 (2002).

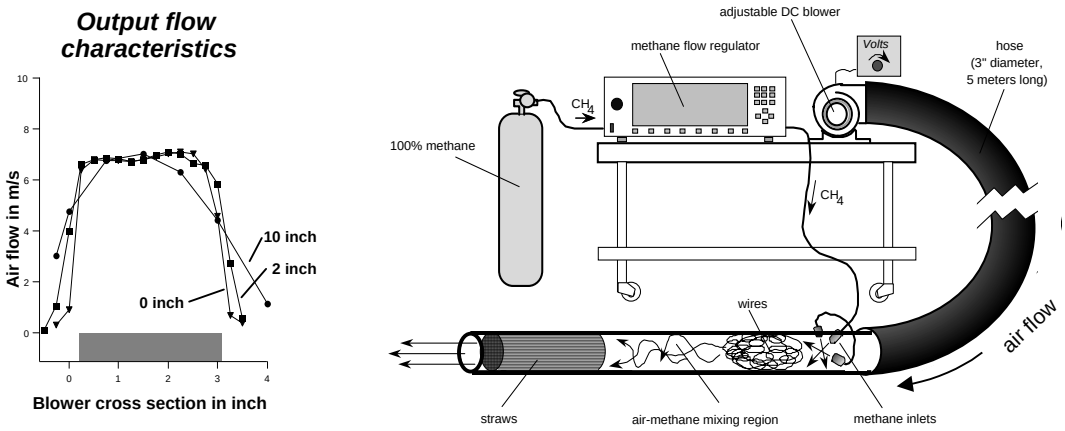

Figure 8. Illustration of plume generator.

Figure 9 and Figure 10 demonstrate detection of methane plumes at 30-m and 100-m standoff distances, respectively. The instrument stares at a fixed spatial location; therefore, to demonstrate gas detection, we translated the gas plume into and then out of the instrument's field-of-view. Each waveform point represents the ratio of the return energies of "on" pulses to that of "off" pulses. Because the laser is generating pulses at 30 kHz, 30,000 ratioed data points are acquired in the 2-second time spans displayed. We display the data simulating both of the acquisition scenarios discussed in Section 5: the raster scanning scenario and the single line-of-sight scenario. We simulate these acquisition scenarios by averaging the data in appropriately spaced temporal bins. The improved noise reduction for the single line-of-sight results from increased averaging allowed by the lower acquisition speed. Because the laser acquires an on/off measurement at a rate of 15 kHz, the number of such data points averaged for the scanning scenario is 15,000 Hz /2140 Hz = 7, while the number of data points averaged for the single line-of-sight is 15,000 Hz / 107 Hz = 140. It is worth noting that the noise level of the averaged data at a standoff distance of 100-m is not significantly worse than that at 30 m. However, the baseline value of S_{on}/S_{off} is less for the longer standoff distance of 100 m. Ambient methane absorbs a greater portion of the on-wavelength at 100 m, decreasing the mean value of the ratioed signal.

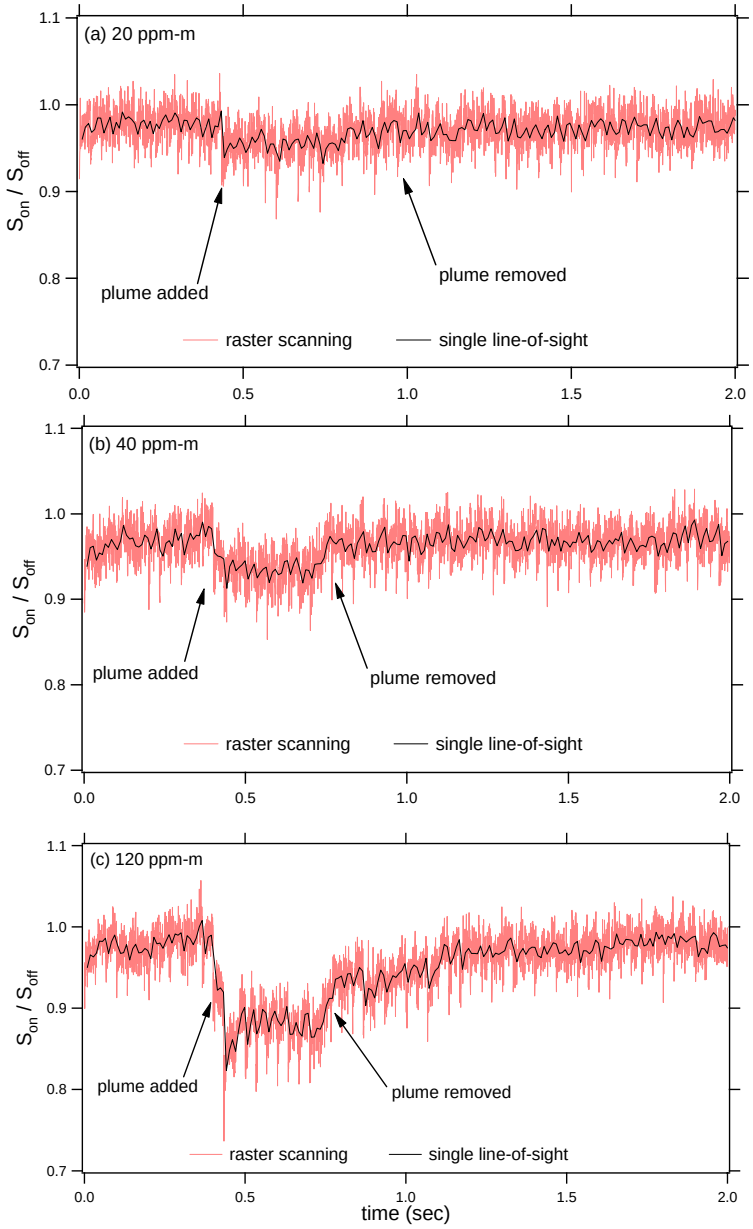

Figure 9. Demonstration of methane-plume detection at a 30-m standoff distance for three pathlength-integrated concentrations: (a) 20 ppm-m, (b) 40 ppm-m, and (c) 120 ppm-m. For each plume, the raster scanning and single line-of-sight scenarios are displayed. The detection limit for raster scanning is estimated to be 40 ppm-m.

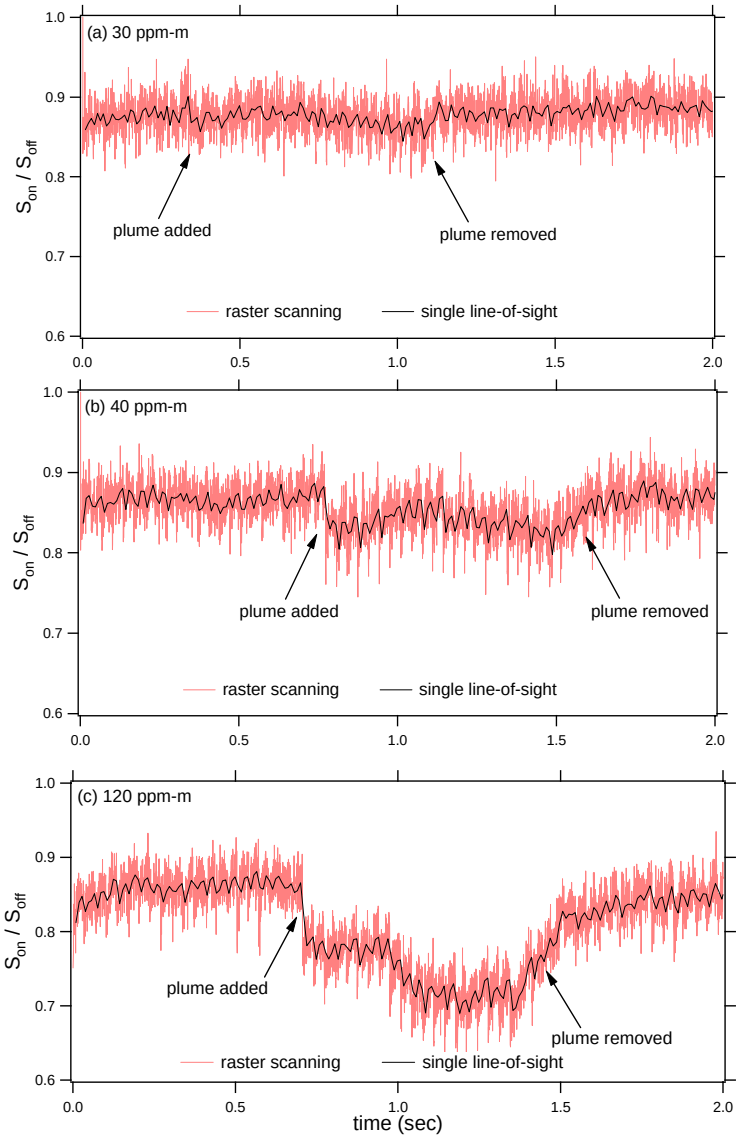

Figure 10. Demonstration of methane-plume detection at a 100-m standoff distance for three pathlength-integrated concentrations: (a) 30 ppm-m, (b) 40 ppm-m, and (c) 120 ppm-m. For each plume, the raster scanning and single line-of-sight scenarios are displayed. The detection limit for raster scanning is estimated to be 40 ppm-m.

8. Proposed System Improvements

The detection limit for the raster scanning scenario at a 100-m standoff distance was estimated to be 40 ppm-m, about an order-of-magnitude larger than that predicted by our previous system modeling. The acquired time-series of data pointed to two major factors limiting the system performance. Firstly, it was apparent that we were not obtaining the expected 1% absorption per 1 ppm-m of methane (see Figure 2). For example, we expected that a 20 ppm-m plume should absorb approximately 20% of the "on" pulse, whereas we are seeing only about 3% absorption through 20 ppm-m of methane (see Figure 9(a)). The laser source is not spectrally matched to the absorption feature, decreasing the contrast between the "on" and "off" pulses, thus degrading the system performance. Also evident from the raw data was a significant noise component occurring at 30 Hz, corresponding to 500 ratioed data points. Because averaging on short time scales does not reduce this noise component, such a noise source ultimately limits the sensitivity of the measurement. We believe this noise source originates from a software update, occurring every 500 points, which affects the OPG diode seed current. The software should be updated to eliminate this noise source.

9. Future Airborne Testing

Before airborne testing, we would have to harden and integrate the system. Power supplies and electronic driver circuits require integration for a fieldable instrument. The light source, currently constructed from individual commercial optical mounts, should be replaced with a glue-down optical system.[5] The number of spring-loaded positioning devices should be reduced, and those that are required should provide secure locking.

For initial airborne test of the instrument, Ross Aviation in Albuquerque operates a number of aircraft for both freight and passenger use for the DOE. Among the DOE aircraft are two DeHaviland Twin Otters, a two engine, 20-passenger, short-takeoff-and-landing aircraft (see Figure 11). The Twin Otter has been used extensively for a variety of Sandia and other national lab research including atmospheric sampling, synthetic aperture radar development, a projectile dropping platform, airborne control platform for UAV development, airborne photography, as well as many other applications. FAA approvals have been obtained for flying the aircraft with the cargo doors removed. In this configuration, remote sensing instrumentation packages can be easily positioned inside the aircraft and oriented to look obliquely at the ground through the side door opening. The Twin Otter also has a bottom viewing port such that an instrumentation system could also be palletized and configured for a downward looking orientation. The Twin Otter is available for a $1000/day base-use fee with additional charges of $500/hour incurred for flight time. The approximate costs for installation of a palletized instrument and 20 hours of flight time, assuming an experiment duration of three weeks, would be ~$25K.

[5] U.-B. Goers, K. Armstrong, R. Sommers, T. J. Kulp, D. A. V. Kliner, S. Birtola, L. Goldberg, J. P. Koplow, and T. G. McRae, "Development of a compact gas imaging sensor employing a cw fiber-amp-pumped PPLN OPO," Conference on Lasers and Electro-Optics 2001 Technical Digest, Baltimore, MD (2001), p. 521.

Figure 11. Twin Otter research aircraft